Base Transit Time Modeling of Gaussian-Doped SiGe HBT Considering Field-Dependence of Mobility

S. M. M. Islam[1], Y. Arafat[2], M. Z. R. Khan[2], M. I. B. Chowdhury[1,*]
[1]*Department of Electrical and Electronic Engineering, United International University, Dhaka*
[2] *Department of Electrical and Electronic Engineering, Bangladesh University of Engineering and Technology, Dhaka*
*(E-mail: *ibchy@eee.uiu.ac.bd)*

Abstract—This work assesses the effects of field-dependence of the carrier mobility on the base transit time of an npn SiGe hetero-junction bipolar transistor (HBT) with its base heavily doped with Gaussian type doping profile. Three types of Ge dosing, namely, box, trapezoidal and triangular profiles of SiGe HBT is represented by a generalized trapezoidal Ge-dosing profile. An analytical model has been developed considering this field-dependence. The model also includes the various effects caused by the non-uniformity of the base doping profile and also, of the Ge-content in the base. The model applicability has been extended from the low-injection level to the moderate-injection level by applying the concept of perturbation theory. The simulation results of the developed model show that the field-dependence of the carrier mobility increases the base transit time considerably. This increase in the transit time is found higher in the SiGe HBTs in comparison with the Si BJTs (no Ge dosing). Among the three Ge dosing profiles of Gaussian doped SiGe HBT, this increase is observed as the highest for triangular one under all level of injections. Model results also show that the increase in the transit time decreases as the peak Ge-fraction increases for a triangular Ge-dosing profile and of uniform, exponential and Gaussian base doping profiles, this increase is found the largest for Gaussian one. All these results are, therefore, crucial for designing low transit time and corresponding high frequency SiGe-HBT design.

Keywords—*Base Transit Time; SiGe-HBT; Moderate-level Injection; Gaussian Doping Profile; Trapezoidal Ge-Dosing Profile; Field Dependence of Carrier Mobility.*

I. INTRODUCTION

In comparison with homojunction Si bipolar transistors, heterojunction bipolar transistors (HBTs) possess higher cutoff frequency (f_T), higher maximum frequency of operation (f_{max}), better noise figure, lower base resistance and lower emitter current crowding. Most HBTs are formed using III-V semiconductor like AlGaAs, InP etc, Recently, as their efficient alternative [1,2] and also, of mature process technology, SiGe-based HBTs become popular in the Radio Frequency Integrated Circuits (RFIC) [3]. In order to obtain improved frequency response, the base of these SiGe HBTs are usually doped heavily and non-uniformly. Germanium (Ge) is dosed in the base to reduce the bandgap narrowing effects [4] and to increase the carrier mobility, which leads further improvement in the device performance. However, Ge-dosing causes strain in the base which may degrade the device performance. Making the base width less than a critical value [5], this detrimental effect can be reduced to tolerable limit.

Unity-gain-bandwidth cutoff frequency (f_T) described the high frequency performance of bipolar transistors and can be determined from the total transit time (τ_{ec}). At moderate or high current levels, the base transit time (τ_B) comprises more than 70% of τ_{ec} [6] and hence, leads the high frequency performance of BJTs. Reduction of this τ_B to obtain high frequency performance can be made possible in SiGe HBTs by applying non-uniform doping profile as well as using Ge-content in the base. Additionally, use of heavy level of doping in the base leads to higher current. However, heavy and non-uniform base doping introduces various non-ideal effects which includes bandgap narrowing effects, doping and field dependence of carrier mobility, velocity saturation effects etc. Therefore, the accurate determination of τ_B requires inclusion of all these effects in its accurate modeling. In the literature, numerous researchers [7-9] developed various models to determine τ_B. Since inclusion of all these effects leads to an analytically intractable differential equation, these models failed to include all these effects and also, have been developed based on numerical methods. Basu [10] developed an analytical model of τ_B, where he considered the doping dependence of the bandgap narrowing effect. But this did not consider the injection-level dependence of the base transit time. Including the injection-level dependence, Arafat *et al.* [11] developed an analytical model which considered the doping and field dependence of the carrier mobility as well. However, this model has been developed for exponential base doping profile. For the Gaussian doped base, S. M. M. Islam *et al.* developed analytical models [12-14]; where, [12] is applicable for low injection level condition, [13] extended this model to high-injection level condition and [14] provided a detailed physics-based analysis applicable for all-levels of injection. However, all of these models have one thing in common i.e. they all neglected the field-dependence of the carrier mobility. The objective of this work is, therefore, firstly to develop an analytical model applicable for all-injection levels and including the field-dependence of carrier

mobility and then, secondly to investigate the effects aiming to provide a better physical insight.

The work is divided in two main sections. In Section II, the analytical development of the base transit time modeling has been gradually described. Section III presents the results as well as their physics-based analysis for carrying out the simulation of the proposed model for three shapes of Ge-profile along with Si-homojunction BJT. A detailed comparative analysis of the proposed model with the model developed in [14] is also presented in this section. The conclusion section finally briefs the outcome of this work.

II. ANALYSIS

The analysis carried out in this work assumes that 1) the electron transport in the base is one dimensional (1D), 2) the thermal equilibrium minority carrier concentration is negligible because of heavy doping level, 3) quasi-charge neutrality condition is prevailed throughout the base region, 4) majority carrier density flowing through the base is zero and 5) recombination in the base can be neglected as the base region under consideration is very thin (less than 100 nm). For 1D assumption, the carrier mobility and the electric field can be considered as function of x only. For the second assumption, $n_0 << N_B$ where n_0 and N_B are the minority electron concentration and the base doping level respectively. The third assumption leads the Poisson's equation to be redundant and hence, electric field in the base can be calculated using the conventional zero-majority current assumption (fourth assumption). Neglect of recombination makes the minority electron current flowing through the base as constant. However, physical models are required for the carrier mobility, the band-gap narrowing effects and the velocity saturation to incorporate the effects owing to the non-uniformity and the heavy level of doping as well as the presence of Ge-content. All these equations and physical models (except the field dependence of the carrier mobility) along with the base doping and Ge-dosing profiles can be summarized from [14] as below:

Basic Equations:

$$\tau_B = -\frac{q}{J_C}\int_0^{W_B} n(x)dx \tag{1}$$

$$J_n = qn(x)\mu_n(x)E(x) + qD_n(x)\frac{dn(x)}{dx} \tag{2}$$

$$E(x) = \frac{kT}{q}\left\{\frac{1}{p(x)}\frac{dp(x)}{dx} - \frac{1}{n_{ie}^2(x)}\frac{dn_{ie}^2(x)}{dx}\right\} \tag{3}$$

Where τ_B is the base transit time, W_B is the base width, n(x) and p(x) are the minority electron concentration and the majority hole concentration respectively, n_{ie} and E(x) are the effective intrinsic carrier concentration and the electric field respectively (both includes the bandgap narrowing effects due to heavy doping and Ge-content), $J_n(x)$ is the electron current density flowing through the base, J_C [= $J_n(W_B)$] is the collector current density, $V_T = \frac{kT}{q}$ is the thermal voltage and μ_n, D_n are the electron mobility and the diffusivity respectively.

Base Doping Profile:

Base Doping profile is Gaussian and can be given as

$$N_B(x) = N_B(0)e^{-mx^2} \tag{4}$$

where, $m = \frac{1}{2\sigma^2}$, $\sigma = \frac{W_B}{\sqrt{2\ln\left[\frac{N_B(0)}{N_B(W_B)}\right]}}$, $N_B(0)$ and $N_B(W_B)$ are the doping concentration at the base-emitter junction (x = 0) and at the base-collector junction ($x=W_B$) respectively.

Ge-Dosing Profile:

The generalized trapezoidal Ge-dosing profile is

$$y(x) = m_{Ge}x + y_E = \frac{y_C - y_E}{W_B}x + y_E \tag{5}$$

Eqn. (5) becomes a triangular profile if $y_E = 0$ and a box profile if $y_C = y_E$.

Physical Models:

$$\mu_{n0} = \mu_{n0}(0)e^{-m_1x^2} \tag{6}$$

$$n_{ie}^2(x) = n_{ie}^2(0)e^{m_3x - m_2x^2} \tag{7}$$

$$v_s = \left[\frac{0.342}{0.342 + y_{av}(1-y_{av})}\right]v_{s,Si} \tag{8}$$

where

$$\mu_{n0}(0) = (1+3y_{av})\mu_n(0)\left[\frac{N_B(0)}{N_{m,ref}}\right]^{-\gamma_1}$$

$$n_{ie}^2(0) = n_{i0,Si}^2\gamma_r e^{\gamma_3 y_E}\left[\frac{N_B(0)}{N_r}\right]^{\gamma_2},$$

Eqns. (6), (7) and (8) represent the physical models for low-field mobility, effective intrinsic concentration and saturation velocity respectively for the SiGe-HBT with Gaussian-doped base, $m_1 = m\gamma_1$, $m_2 = m\gamma_2$, $m_3 = m_{Ge}\gamma_3$ and the constants γ_1, γ_2, γ_3, γ_r, $N_{m,ref}$, N_r, $n_{i0,Si}$, $v_{s,Si}$ and $\mu_n(0)$ are defined in [14]. Since this work considers the field-dependence of the carrier mobility in the mobility, it is necessary to include the widely known Cauchey-Thomas-Thornber's mobility model in the analysis. Since this model is complicated, a simplified model used in [15] is employed here and can be given as

$$\mu_{n,} = \frac{\mu_{n0}}{1 + \frac{a_e}{qv_s}\left|\frac{E(x)}{V_T}\right|} \tag{9}$$

where a_e =0.7743 [15]. Using the Einstein's relation i.e. $\frac{D_n}{\mu_n} = V_T$, the electron mobility can be organized in terms of diffusivity as

$$\frac{1}{qD_n} = \frac{1}{qD_{n0}} + \frac{a_e}{qv_s}\left|\frac{E(x)}{V_T}\right| \tag{10}$$

where

$$\frac{1}{qD_{n0}} = \frac{1}{qD_{n0}(0)} e^{m_1 x^2}$$

A. Model Derivation

Rearranging Eqn. (2), the governing differential equation (DE) of minority electron concentration n(x) can be obtained as

$$\frac{dn(x)}{dx} + \frac{E(x)}{V_T} n(x) = \frac{J_n}{qD_n} \tag{11}$$

Combining with the expression of electric field given by Eqn. (3), the above DE can be organized as

$$\frac{d}{dx}\left(\frac{pn}{n_{ie}^2}\right) = \frac{p}{n_{ie}^2}\frac{J_n}{qD_n} \tag{12}$$

Integrating Eqn. (12) from x = 0 to x and rearranging the terms gives

$$n(x) = \frac{n_{ie}^2}{p}\left[\frac{p(0)n(0)}{n_{ie}^2(0)} + J_n I(x)\right] \tag{13}$$

where

$$I(x) = \int_0^x \frac{p(x)}{qD_n(x)n_{ie}^2(x)} dx$$

Two boundary conditions are required to solve the above-mentioned DE. At x = 0, the electron concentration can be found by using the following relation [16] considering the Webster effect [17]

$$n(0) = \frac{n_{ie}^2(0)}{N_B(0)} e^{\frac{V_{BE}}{V_T}} f_w \tag{14}$$

Where $f_w = \dfrac{1}{0.5 + \sqrt{0.25 + \left[\dfrac{N_B^2(0)}{n_{ie}^2(0)}\right] e^{\frac{V_{BE}}{V_T}}}}$

Considering the velocity saturation at the base-collector junction i.e. at x = W_B [18], another boundary condition can be obtained as

$$J_n = -qv_s n(W_B) \tag{15}$$

Applying these boundary conditions in Eqn. (13) results in

$$J_n = -\frac{\dfrac{n_{ie}^2(W_B)}{n_{ie}^2(0)}\dfrac{p(0)}{p(W_B)}}{\dfrac{1}{qv_s} + \dfrac{n_{ie}^2(W_B)}{p(W_B)} I(W_B)} \tag{16}$$

$$n(x) = -J_n \frac{n_{ie}^2}{p}\left[\frac{p(W_B)}{n_{ie}^2(W_B)}\frac{1}{qv_s} + I(W_B) - I(x)\right] \tag{17}$$

Under low injection (LI) condition n(x) << $N_B(x)$ and hence, p(x) ≈$N_B(x)$. Therefore, the low-injection solution of Eqn. (17) can be obtained as

$$n_l(x) = -J_{nl}\frac{n_{ie}^2}{N_B}\left[\frac{N_B(W_B)}{n_{ie}^2(W_B)}\frac{1}{qv_s} + I_l(W_B) - I_l(x)\right] \tag{18}$$

$$J_{nl} = -\frac{\dfrac{n_{ie}^2(W_B)}{n_{ie}^2(0)}\dfrac{N_B(0)}{N_B(W_B)}}{\dfrac{1}{qv_s} + \dfrac{n_{ie}^2(W_B)}{N_B(W_B)} I_l(W_B)} \tag{19}$$

where, $I_l(x) = \int_0^x \frac{N_B(x)}{qD_{nl}(x)n_{ie}^2(x)} dx$ and the subscript 'l' denotes the low-injection value. However, for moderate injection-level condition, n(x) is comparable with $N_B(x)$ and hence, makes Eqn. (17) analytically intractable. As suggested in [16], this intractability problem can be resolved by using the concept of perturbation theory. Suzuki *et. al* [16] suggested that the electron concentration under moderate injection level condition, n(x) is perturbed a little [δn(x)] by the modulated electric field owing to increased level of injection from its extended low-level concentration, $n_m(x)$ to incorporate Webster effect [17], an effect that occurs under higher-level injection condition. Mathematically, this implies that

$$n_m(x) = n_l(x) f_w$$
$$n(x) = n_m(x) + \delta n(x)$$
$$p(x) = n_m(x) + \delta n(x) + N_B(x) \approx n_m(x) + N_B(x) \tag{20}$$

where f_w is introduced to incorporate Webster effect, quasi-charge neutrality condition is employed and the deviation δn(x) must be << $n_m(x)$ + $N_B(x)$ instead of << $n_m(x)$ for the sake of derivational accuracy. This requirement, however, sets the model validity prior to the onset of the Kirk effect [19], a phenomenon considered to be the onset of high injection level condition. Using Eqn. (20), the moderate-injection level solution of n(x) can be obtained from Eqn. (17) as

$$n(x) = -J_n \frac{n_{ie}^2}{n_m + N_B}\left[\frac{n_m(W_B) + N_B(W_B)}{n_{ie}^2(W_B)}\frac{1}{qv_s} + I_m(W_B) - I_m(x)\right] \tag{21}$$

$$J_n = -\frac{\dfrac{n_{ie}^2(W_B)}{n_{ie}^2(0)}\dfrac{n_m(0) + N_B(0)}{n_m(W_B) + N_B(W_B)}}{\dfrac{1}{qv_s} + \dfrac{n_{ie}^2(W_B)}{n_m(W_B) + N_B(W_B)} I_m(W_B)} \tag{22}$$

where, $I_m(x) = \int_0^x \frac{n_m(x) + N_B(x)}{qD_n(x)n_{ie}^2(x)} dx$. Finally, the base transit time can be calculated from Eqn. (1), by putting J_C = J_n and integrating n(x) given by Eqn. (21) from x = 0 to x.

III. RESULTS AND DISCUSSIONA

The simulation results of the propose model developed in this work are presented and analyzed in this section. The results are compared with the model that neglects the effect of the field dependence of the carrier mobility. The npn SiGe

HBT is doped with Gaussian doping profile having doping concentrations of 5×10^{18} cm^{-3} and 1×10^{17} cm^{-3} at the base-emitter (B-E) and the base-collector (B-C) junctions i.e. at i.e. x = 0 and x = W_B respectively. Three shapes of Ge-dosing profile are chosen, namely, box, trapezoidal and triangular with Ge-fraction at the emitter-side (x = 0) as 0%, 5% and 10% respectively and peak Ge-fraction of 10% at the collector side (x = W_B). In order to get better insight, the results are also compared with Si BJT that has no Ge dosing. The base width is chosen as 100 nm.

Fig. 1 shows the space-dependency of the electron mobility in the base. From this figure it is obvious that the inclusion of field dependency decreases the carrier mobility. This decrease is the most for the triangular profile, the least for the box profile and in-between for the trapezoidal profile and for the Si BJT. This is simply because of the fact that the electric field is the highest for triangular, the lowest for box and in-between for trapezoidal and no Ge-profile [Eqn. (10)]. The differences in mobility observed from Fig. 1 under no-field condition for all four cases can be attributed to the different values of average Ge dosing, y_{av}. Indeed, the higher the y_{av}, the higher the mobility. The y_{av} is the highest for the box, the lowest for the triangular and in-between for the trapezoidal dosing profile, whereas, for Si BJT it is zero. Therefore, the mobility under no field condition can be ordered in descending order as box, trapezoidal, triangular and no Ge profile.

Since, the electric field introduced in the base sweeps out the minority electrons stored in the base to the collector, the higher is the electric field, the quicker the sweeping of electrons resulting in less storage of electrons in the base and also causes the higher current to flow towards the collector. Therefore, the lowest and the highest minority carrier concentrations are observed in Fig. 3 and also, the highest and the lowest current densities are observed in Fig. 2 for the triangular dosing profile and the box profile respectively. However, since field dependency decreases the carrier mobility, the minority concentrations in Fig. 3 and the current densities in Fig. 2 are observed to increase and decrease respectively in all cases when field-dependent carrier mobility is considered. The level of decrease is the highest for the triangular profile and the lowest for the box profile, as the mobility degradation is of the same level for these profiles. Similar reasoning can be applied for the no-Ge case i.e. for Si BJT.

Fig. 4 shows the effect of the field dependence of the carrier mobility on the electric field acting on the minority electrons throughout the base region for the base-emitter voltage (V_{BE}) of 0.87 V. Since the generalized trapezoidal Ge-dosing profile with the peak at the collector side and the minimum at the base side aids the electric field caused by the Gaussian doping profile, the electric field increases if the slope of dosing profile increases. Therefore, with the triangular dosing the electric field is maximum (the slope of dosing is the highest) and with box dosing the electric field is minimum (the slope is zero). These expected results are observed from Fig. 4. These results are also consistent with those observed in the works [13,14].

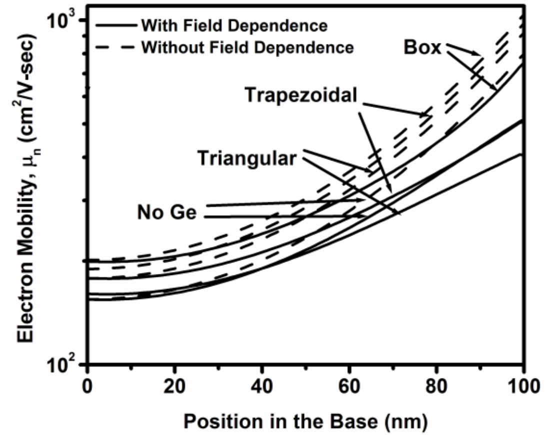

Fig. 1. Minority Electron mobility in the base for different shape of Ge profiles. Here V_{BE} = 0.87 V.

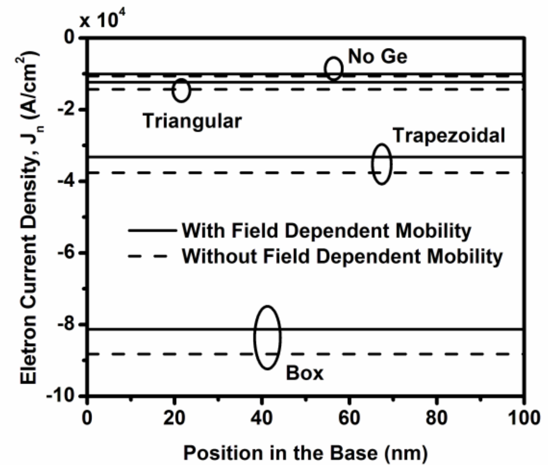

Fig. 2. Minority Electron current density in the base for different shape of Ge profiles. Here V_{BE} = 0.87 V.

Fig. 4 also shows that electric field with field dependence case in comparison with that with no-field dependence case is lower near the B-E junction for most part of the base, but becomes higher close to the B-C junction. This can be explained with the help of the Fig. 1 and 3. A close scrutiny of the plots shown in Fig. 3 reveals that minority electron concentration for the field dependence case is higher than that for no-field dependence case in most part of the base region and is lowered down near the B-C junction. Since the mobility with field dependence is lower than that with no-field dependence, electrons in the former case becomes sluggish to leave the base region and hence, are stored in the base region in larger number causing an increase in the concentration in the base and a decrease in the concentration gradient. Therefore, electric field becomes lower in this region of the

base as observed in Fig. 4. However, as an electron moves from the B-E junction towards the B-C junction, the velocity of this electron increases and reaches the saturation velocity near the B-C junction. Since the electron mobility monotonically increases throughout the base region (Fig. 1), the velocity saturation near the B-C junction results in a decrease (as observed in Fig. 4) in the electric field therein. Again, since the mobility is degraded in case of field-dependence consideration (Fig. 1), the electric field for this case becomes higher near the B-C junction (Fig. 4). This also explains the lowering of n(x) near the B-C junction (Fig. 3) for the field-dependence case compared to the no-field dependency case.

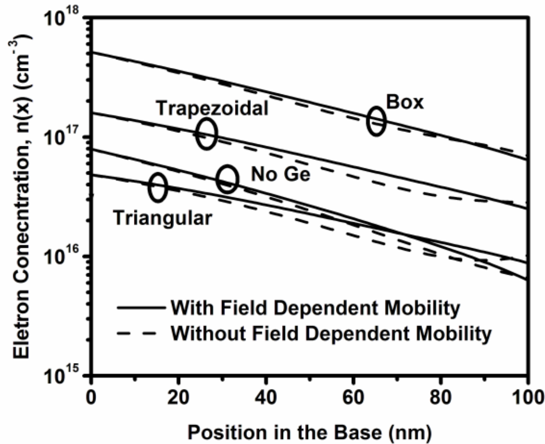

Fig. 3. Minority electron concentration in the base for different shape of Ge profiles. Here V_{BE} = 0.87 V.

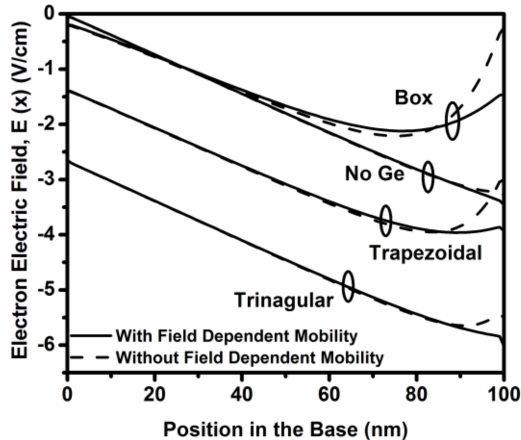

Fig. 4. Variation of electric field in the base for different shape of Ge profiles. Here, V_{BE} = 0.87 V.

The functional relation between the collector current density and the base emitter voltage (V_{BE}) is plotted in Fig. 5. For lower V_{BE}, the plots for all cases are linear in logarithmic scale, but as V_{BE} increases the slope of the plots starts to decrease. This is due to the entering into the moderate injection level condition for which linearity in the log scale no longer exists. Therefore, from Fig. 5 it can be argued that the triangular dosed HBT and the Si BJT enter the MI condition for V_{BE} > 0.90 V, whereas, the box dosed and the trapezoidal dosed HBTs enter for V_{BE} > 0.85 V. Since the electron current density in the base, which is the collector current density (J_C) for the present analysis, is lower for the field-dependence case than for the no-field dependence case, J_C is seen lower for all cases in Fig. 5 when the field-dependence of the carrier mobility is taken into consideration. These same results are also seen in [4].

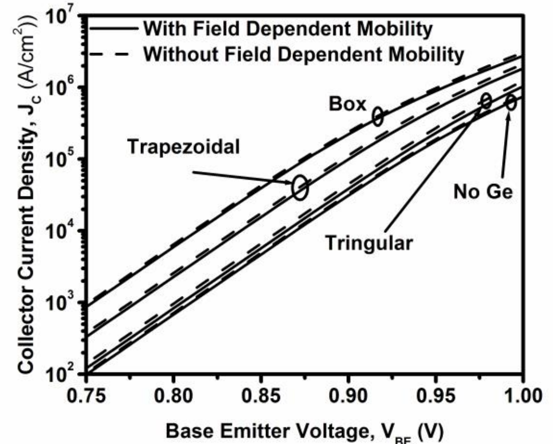

Fig. 5. Collector Current densities vs. base-emitter voltage for different shape of Ge profiles.

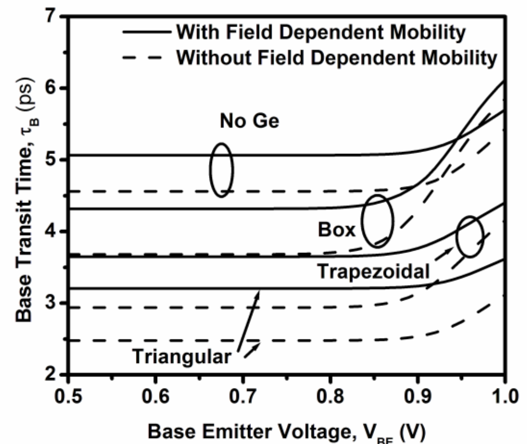

Fig. 6. Base transit time vs. base-emitter voltage for different shape of Ge profiles.

Fig. 6 plots of the base transit time (τ_B) to illustrate its functional relationship with the base emitter voltage (V_{BE}), for different profiles of Ge content in the Gaussian-doped base. Since field dependence consideration reduces the carrier mobility and hence, increases the carrier concentration and decreases the collector current density, the base transit with the field-dependence consideration is expected to increase. Fig. 6 complies with this expectation and hence, τ_B for field-dependent mobility consideration for all cases are higher. Fig. 6 also shows that Si HBT is worse than the SiGe HBT in terms of minimum-τ_B consideration and introduction of Ge dosing

can reduce the τ_B considerably. Another observation from this figure is that the box-dosed SiGe HBT enters the high injection condition at a lower V_{BE} than the trapezoidal- and triangular-dosed SiGe HBT. This is due to the slope of Ge-dosing profile, which increases the electric field in the base and hence, increases the V_{BE} for which MI condition occurs.

Fig. 7 presents a comparative demonstration of SiGe HBTs having three types of doping profile, namely, Gaussian, exponential [13] and uniform doping profile [7] for $V_{BE} = 0.9$ V. All these HBTs have a base width of 45 nm, have same boundary conditions of base doping as in [13] (exponential doping profile with peak doping concentration of 8×10^{18} cm^{-3} and the logarithmic slope of 3.5) and are Ge-dosed with triangular profile ($y_E = 0$). Form Fig. 7, it is evident that τ_B is the lowest for the Gaussian, highest for the uniform and in-between for the exponential doping profile and decreases as the peak Ge-fraction increases, whether the field dependence is considered or not. This is because of the fact that the doping gradient is the highest for the Gaussian doping, lowest (zero) for the uniform doping and in-between for the exponential doping profile. For the same reasoning, it is also observed from Fig. 7 that the field-dependence consideration increases the transit time in all the three cases and the increase is the highest for the Gaussian doped base.

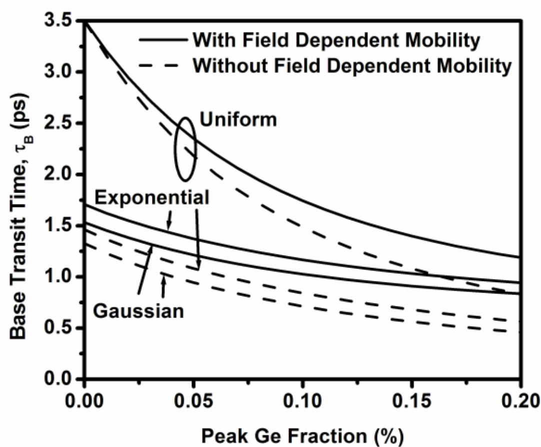

Fig. 7. Base transit time vs peak Ge fraction in the triangular profile dosed SiGe HBT for uniform, exponential and Gaussian base doping profile.

IV. CONCLUSION

In this work a thorough physics-based analysis of the base transit time of SiGe HBT considering the effects of field dependence of the minority carrier mobility has been presented. The base of the npn SiGe HBT is heavily doped with Gaussian profile and dosed with a generalized trapezoidal Ge profile with a motivation of increasing field in the base and corresponding reduction of base transit time. An analytical base transit time model has been developed considering the field dependence of the carrier mobility along with other effects owing to the non-uniformity of both the doping and the dosing profiles. Simulation results using the developed model shows that the field dependence consideration has significant effects on the minority carrier distribution, electric field profile, mobility profile and minority current density throughout the base region under moderate injection level condition. These effects lead to significant decrease on the collector current density and hence, on the base transit time even under the high-bias level. Dominant effects have been observed for triangular dosing profile for Gaussian doped base and Gaussian doping profile for triangular dosing profile, since in either case electric field is found to be greatest among the various types of dosing profiles (box, trapezoidal and triangular) and of doping profiles (uniform, exponential and Gaussian) respectively. Therefore, field-dependence of the carrier mobility should be included in the base transit modeling.

REFERENCES

[1] N. Zerounian, F. Aniel., B. Barbalat, P. Chevalier, and A. Chantre, "500 GHz cutoff frequency SiGe HBTs", Electronics Letters, vol. 43, pp. 774-775, July 2007.

[2] Z. Xu, G. Niu, L. Luo, P. S. Chakraborty, P. Cheng, D. Thomas, and J. D. Cressler, "Cryogenic RF Small-Signal Modeling and Parameter Extraction of SiGe HBTs", IEEE Topical Meeting on Silicon Monolithic Integrated Circuits in RF Systems, SiRF'09, pp. 1-4, 2009.

[3] K. Lee, D. H. Cho, K. W. Park, and B. Kim, Improved VBIC Model for SiGe HBTs With a Unified Model of Heterojunction Barrier Effects, IEEE Tran. on Electron Devices, vol. 53(4), p. 743, 2006.

[4] M. K. Das, N. R. Das, and P. K. Basu, "Effect of Ge content and profile in the SiGe base on the performance of a SiGe/Si HBT", Microwave and Optical Technology Letters, vol. 47, pp. 247-254, 2005.

[5] S. C. Jain, "Germanium-Silicon Strained Layers and Heterostructures", Academic Press, Inc. USA, 1994.

[6] Mandal S. K., Marskole G. K., Chari K. S., and Maiti C. K., Transit time components of a SiGe-HBT at low temperature, Proc. 24th International Conference on Microelectronics, Nis, Serbia and Montenegro, pp. 315-318, 2004.

[7] Patri V. S. and Kumar M. J., Profile Design Considerations for minimizing base transit time in SiGe HBT's, IEEE Trans. on Electron Devices, vol. 45, pp. 1725-1731, 1998.

[8] Tang Z. R., Kamins T., and Salama C. A. T., Analytical and experimental characteristics of SiGe HBT with thin á-Si : H emitters", Solid-State Electron., vol. 38, pp. 1829-1834, 1995.

[9] Kwok K. H. and Selvakumar C. R., Profile design considerations for minimizing base transit time in SiGe HBTs for all levels of Injection before onset of Kirk effect, IEEE Tran. on Electron Devices, vol. 48, pp. 1540-1549, 2001.

[10] Basu S., Analytical Modeling of Base Transit Time of SiGe HBTS Including Concentration Dependent Bandgap Narrowing Effect, Journal of Electronic Science and Technology, vol. 8, no. 2, pp. 140-143, 2010.

[11] Arafat Y., Khan M. Z. R. and Hassan M. M. S., Analytical Modeling of Base Transit Time for a Si1-xGex Heterojunction Bipolar Transistor, IEEE International Conference of Electron Devices and Solid-State Circuits, EDSSC 2009, Xi'an, China, pp. 358-361, 2009.

[12] Islam S. M. M., Chowdhury M. I. B., Arafat Y., Khan M. Z. R. and Hassan M. M. S., Base Transit Time of a Heterojunction Bipolar Transistor with Gaussian Doped Base, IEEE International Conference on Electrical and Computer

Engineering, ICECE 2010, Dhaka, Bangladesh, pp. 127-130, 2010.

[13] Islam S. M. M., Chowdhury M. I. B., Arafat Y. and Khan M. Z. R., Base Transit Time of a Heterojunction Bipolar Transistor (HBT) with Gaussian Doped Base Under High-Level of Injection, IEEE International Conference on Devices, Circuits and Systems, ICDCS 2012, Coimbatore, India, pp. 114-118, 2012 .

[14] Islam S. M. M., Chowdhury M. I. B., Arafat Y. and Khan M. Z. R., Physics-Based Analysis of Base Transit Time of SiGe HBT with Gaussian Doped Base, ISTP Journal of Research in Electrical and Electronics Engineering (ISTP-JREEE)-1st International Conference on Research in Science, Engineering & Management (IOCRSEM 2014), pp. 80-86, 2014.

[15] M. M. S. Hassan and M. W. K. Nomani, "Base transit time model considering field dependent mobility for BJTs operating at high-level injection", IEEE Tran. on Electron Devices, vol. 53, pp. 2532-2539, 2006.